# SUPPORTING INFORMATION

## Kinesin-2 heterodimerization alters entry into a processive run but not stepping within the run

Sean M. Quinn[1,a], Daniel P. Howsmon[2,a#], Juergen Hahn[2,3*], Susan P. Gilbert[1*]

Department of Biological Sciences[1], Department of Chemical & Biological Engineering[2,], and Department of Biomedical Engineering[3], Center for Biotechnology and Interdisciplinary Studies, Rensselaer Polytechnic Institute, Troy, NY 12180

Running title: Kinesin-2 KIF3AC and KIF3AB stepping

THE SUPPORTING INFORMATION CONTAINS:

3 Tables
2 Figures
Computational modeling Approach and Methods
Supporting References

| KIF3AC Parameter Constraints | | | | |
|---|---|---|---|---|
| **Transition** | **Condition** | **Description** | **Valid (Yes/No)** | **Reason** |
| Microtubule Association (E0-E1) | 1 | $k_{1a} + k_{1c} = k_{1ac}$ | Yes | Microtubule association by KIF3A and KIF3C are interdependent. |
| | 2 | $(k_{1a} + k_{1c})/2 = k_{1ac}$ | No | |
| ADP Release/mantATP Binding (E1-E2) | 3 | $k_{2a} + k_{2c} = k_{2ac}$ | No | ADP release by KIF3A is independent of ADP release by KIF3C. |
| | 4 | $(k_{2a} + k_{2c})/2 = k_{2ac}$ | Yes | |
| Steps from Isomerization to Dissociation/mantATP Binding (E2-E5) | 5 | $k_{3a} + k_{3c} = k_{3ac}$ | No | When the KIF3A and KIF3C pathways proceed through transitions E2-E5 are independent. |
| | 6 | $(k_{3a} + k_{3c})/2 = k_{3ac}$ | Yes | |

**Table S1 Assessment of the validity of alternative KIF3AC model parameter constraints**

**Condition 1:** The heterodimeric KIF3AC microtubule association parameter is represented by the sum of the KIF3A and KIF3C parameters was accepted as valid. A single KIF3A or KIF3C site per heterodimer can associate with the microtubule during entry into the processive run. The association of a motor with the microtubule depletes the concentration of unoccupied microtubule sites and total possible KIF3A or KIF3C sites that can collide with the microtubule. Because of the interdependence of KIF3A on KIF3C during microtubule association, a constraint was imposed where the sum of the KIF3A and KIF3C microtubule association parameters ($k_{1a}$ and $k_{1c}$) equals the KIF3AC rate constant of 6.6 $\mu M^{-1}s^{-1}$. For the parameter estimation, parameter $k_{1a}$ was selected for estimation, and the constraint was used to determine the value for parameter $k_{1c}$.

**Condition 2:** The heterodimeric KIF3AC microtubule association rate constant is represented by the average of the KIF3A and KIF3C parameters is NOT valid. KIF3A microtubule association is not independent of KIF3C. A single KIF3A or KIF3C site per heterodimer can associate with the microtubule during entry into the processive run. The association of a motor with the microtubule depletes the concentration of unoccupied microtubule sites and total possible KIF3A or KIF3C sites that can collide with the microtubule. Because of the interdependence of KIF3A on KIF3C during microtubule association, model condition 2 was eliminated.

**Condition 3:** The heterodimeric KIF3AC rate constant for ADP release and mantATP binding is equal to the sum of the KIF3A and KIF3C parameters is NOT valid. There is no interdependence of ADP release by KIF3A on KIF3C. In other words, each ADP release event by KIF3A is independent of ADP release by KIF3C.

**Condition 4:** The rate constant for ADP release and mantATP binding for heterodimeric KIF3AC is equal to the average of the KIF3A and KIF3C parameters was accepted as valid. There is no interdependence of ADP release by KIF3A on KIF3C. In other words, each ADP release event by KIF3A should not affect the ADP release by KIF3C. For the parameter estimation, a constraint where the average of the ADP release rates for KIF3A and KIF3C was equal to the KIF3AC ADP release rate constant of 42.5 $s^{-1}$ was initially imposed; however, when parameter $k_{2a}$ or $k_{2c}$ was

estimated, there was a hardly noticeable change from their nominal values. Therefore, the parameter values for KIF3A and KIF3C were fixed to rates defined by KIF3AA and KIF3CC of 77.7 $s^{-1}$ and 7.6 $s^{-1}$, respectively, where the average of the rates is ~42.5 $s^{-1}$.

**Condition 5:** The KIF3AC parameter representing the series of steps from mantATP-promoted isomerization through dissociation and subsequent mantATP binding (Fig. 1, E2-E5) is equal to the sum of the rates for the corresponding steps in the KIF3A and KIF3C pathways is NOT valid. When the KIF3A pathway proceeds through combined transitions E2-E5 is independent of when the KIF3C pathway proceeds through transitions E2-E5. This sequence of events in the KIF3A and KIF3C pathways are temporally separated due to the asymmetric hand-over-hand model.

**Condition 6:** The KIF3AC parameter representing the series of steps from mantATP-promoted isomerization through dissociation and subsequent mantATP binding (Fig. 1, E2-E5) is equal to the average of the rates for the corresponding steps in the KIF3A and KIF3C pathways was accepted as valid. When the KIF3A pathway proceeds through combined transitions E2-E5 is independent of when the KIF3C pathway proceeds through transitions E2-E5. This sequence of events in the KIF3A and KIF3C pathways are temporally separated due to the asymmetric hand-over-hand model. For the parameter estimation, a constraint was imposed where the average of the rates for the combined steps of the KIF3A and KIF3C pathways is equal to ~50 $s^{-1}$. Parameter $k_{3a}$ was selected for estimation, and the constraint was used to determine the rate for parameter $k_{3c}$.

| KIF3AC Parameter Values | | | | |
|---|---|---|---|---|
| **Transition** | **Condition** | **Intrinsic Properties Retained (Yes/No)** | **Valid (Yes/No)** | **Reason** |
| Microtubule Association (E0-E1) | 1 | Yes | No | Estimation resulted in similar microtubule association parameters for KIF3A and KIF3C. |
| | 2 | No | Yes | |
| ADP Release/mantATP Binding (E1-E2) | 3 | Yes | Yes | Estimation resulted in only a minor change from the intrinsic KIF3A and KIF3C ADP release rates. |
| | 4 | No | No | |
| Steps from Isomerization to Dissociation/mantATP Binding (E2-E5) | 5 | Yes | Yes | Estimation resulted in the parameter corresponding to KIF3A pathway ($k_{3a}$) faster than the parameter corresponding to the KIF3C pathway ($k_{3c}$). |
| | 6 | No | No | |

**Table S2 Assessment of the validity of alternative model conditions for the catalytic properties of the KIF3AC motor pathways**

**Condition 1:** The intrinsic microtubule association properties of KIF3A and KIF3C are retained is NOT valid. Parameter estimation resulted in KIF3A and KIF3C microtubule association parameters that were similar in rate. See computational modeling approach and methods for further details. The KIF3A microtubule association parameter $k_{1a}$ was slower than its intrinsic microtubule association rate of 5.7 $\mu M^{-1}s^{-1}$, and the KIF3C microtubule association parameter $k_{1c}$ was faster than its intrinsic microtubule association rate of 1 $\mu M^{-1}s^{-1}$. In addition, when the intrinsic microtubule association rates were fixed for KIF3A and KIF3C and downstream parameters were estimated, a parameter in the KIF3A pathway was slower than the parameter for the corresponding step in the KIF3C pathway. KIF3A can only have either faster properties than KIF3C or both heads can have similar properties.

**Condition 2:** The intrinsic microtubule association properties of KIF3A and KIF3C are not retained was accepted as valid. Parameter estimation resulted in KIF3A and KIF3C microtubule association parameters that were similar in rate. The KIF3A microtubule association parameter $k_{1a}$ was slower than its intrinsic microtubule association rate of 5.7 $\mu M^{-1}s^{-1}$, and the KIF3C microtubule association parameter $k_{1c}$ was faster than 1 $\mu M^{-1}s^{-1}$. In addition, when the intrinsic microtubule association rates were fixed for KIF3A and KIF3C and downstream parameters were estimated, a parameter in the KIF3A pathway was slower than the parameter for the corresponding step in the KIF3C pathway. KIF3A can only have either faster properties than KIF3C or both heads can have similar properties.

**Condition 3:** The ADP release and mantATP binding properties of the two heads are retained, was accepted as valid. When an ADP release parameter was included in the parameter set for

estimation, there was no noticeable change in the rates from their nominal values. In addition, when the KIF3A and KIF3C heads were fixed to the same ADP release rate of 42.5 $s^{-1}$ corresponding to KIF3AC, the KIF3A microtubule association parameter was estimated to be significantly slower than that of KIF3C. KIF3A can only either have faster properties than KIF3C or both heads can have similar properties.

**Condition 4:** ADP release and mantATP binding properties are not retained is NOT valid. When the KIF3A and KIF3C heads were fixed to the same ADP release rate of 42.5 $s^{-1}$ corresponding to that of KIF3AC, the microtubule association parameter for KIF3A was estimated to be significantly slower than that of KIF3C. KIF3A can only either have faster properties than KIF3C or both heads can have similar properties.

**Condition 5:** The KIF3A and KIF3C pathways retain their intrinsic properties for the nucleotide-promoted transitions following ADP release and mantATP binding was accepted as valid. When the rates for the nucleotide promoted transitions following ADP release and mantATP binding were fixed to equivalent rates at 50 $s^{-1}$ for the KIF3A and KIF3C pathways, the training and validation mean-squared error values were higher indicating poorer simulation fits to the data. In addition, the estimated microtubule association parameter for KIF3A was slower than that of KIF3C. The KIF3A pathway can only either have faster properties than KIF3C pathway or both can have similar properties. Therefore, the KIF3A and KIF3C pathways must retain their intrinsic catalytic properties for these nucleotide promoted transitions.

**Condition 6:** The KIF3A and KIF3C pathways do not retain their intrinsic properties for the nucleotide-promoted transitions following ADP release and mantATP binding is NOT valid. When the rates for the nucleotide-promoted transitions following ADP release and mantATP binding were fixed to equivalent rates at 50 $s^{-1}$ for the KIF3A and KIF3C pathways, the training and validation mean-squared error values were higher indicating poorer simulation fits to the data. In addition, the estimated microtubule association parameter for KIF3A was slower than that of KIF3C. The KIF3A pathway can only either have faster properties than KIF3C pathway or both can have similar properties. Therefore, the KIF3A and KIF3C pathways must retain their intrinsic catalytic properties for the combined steps E2-E5 in Fig. 1.

| KIF3AB Parameter Values | | | | |
|---|---|---|---|---|
| **Transition** | **Condition** | **Intrinsic Properties Retained (Yes/No)** | **Valid (Yes/No)** | **Reason** |
| Microtubule Association (E0-E1) | 1 | Yes | No | Estimation resulted in microtubule association parameters that were slower than the intrinsic KIF3A and KIF3B rates. |
| | 2 | No | Yes | |
| ADP Release/mantATP Binding (E1-E2) | 3 | Yes | Yes | Simulations resulted in the lowest mean-squared error values and best fits when the intrinsic rates were retained. |
| | 4 | No | No | |
| Steps from Isomerization to Dissociation/mantATP Binding (E2-E5) | 5 | Yes | No | Compared to the KIF3A pathway in the KIF3AC model, parameter estimation resulted in a rate for E2-E5 that was slower at 38 $s^{-1}$. |
| | 6 | No | Yes | |

**Table S3 Assessment of the validity of alternative model conditions for the catalytic properties of the KIF3AB motor pathways**

**Condition 1:** The intrinsic microtubule association properties of KIF3A and KIF3B are retained is NOT valid. When implementing the modeling approach for KIF3AB, the estimated microtubule association parameters for KIF3A and KIF3B were slower than their rates in homodimeric KIF3AA and KIF3BB. In addition, when KIF3A and KIF3B were fixed to their microtubule association rates in KIF3AA and KIF3BB, higher mean-squared error values and poorer fits resulted.

**Condition 2:** The intrinsic microtubule association properties of KIF3A and KIF3B are not retained was accepted as valid. When implementing the modeling approach for KIF3AB, the estimated microtubule association parameters for KIF3A and KIF3B were slower than their rates in homodimeric KIF3AA and KIF3BB. When KIF3A and KIF3B were fixed to their microtubule association rates in KIF3AA and KIF3BB, higher mean-squared error values and poorer fits resulted.

**Condition 3:** KIF3A and KIF3B retain their intrinsic ADP release properties was accepted as valid. When running simulations where the KIF3A and KIF3B ADP release rates were fixed to the KIF3AB ADP release rate of 39.6 $s^{-1}$, the simulations fit the fluorescence transients poorly. However, the lowest mean-squared error values and best simulation fits to the data resulted when KIF3A and KIF3B were fixed to their ADP release rates in KIF3AA and KIF3BB.

**Condition 4:** KIF3A and KIF3B do not retain their intrinsic ADP release properties is NOT valid. When running simulations where the KIF3A and KIF3B ADP release rates were fixed to the KIF3AB rate constant of 39.6 $s^{-1}$, the simulations fit the fluorescence transients poorly. However, the lowest mean-squared error values and best simulation fits to the data resulted when KIF3A and KIF3B were fixed to their intrinsic ADP release rates within KIF3AA and KIF3BB.

**Condition 5:** The rates for the combined series of steps from mantATP promoted isomerization through dissociation and subsequent mantATP binding in the KIF3A and KIF3B pathways are retained is NOT valid. When parameters were estimated in the KIF3AB model, the parameter for the composite transitions in the KIF3A pathway ($k_{3a}$) was much slower than the parameter for the corresponding transitions for the KIF3A pathway in the KIF3AC model. If parameter $k_{3a}$ and $k_{3b}$ are fixed to rates of ~90 $s^{-1}$, simulations result in poorer fits to the fluorescence transients.

**Condition 6:** The rates for the combined series of transitions from the mantATP-promoted isomerization through dissociation and subsequent mantATP binding in the KIF3A and KIF3B pathways are not retained was accepted as valid. When parameters were estimated in the KIF3AB model, the parameter for the combined transitions in the KIF3A pathway ($k_{3a}$) was much slower than the parameter for the corresponding steps for the KIF3A pathway in the KIF3AC model. If parameter $k_{3a}$ and $k_{3b}$ are set to rates of ~90 $s^{-1}$, simulations result in poorer fits to the fluorescence transients.

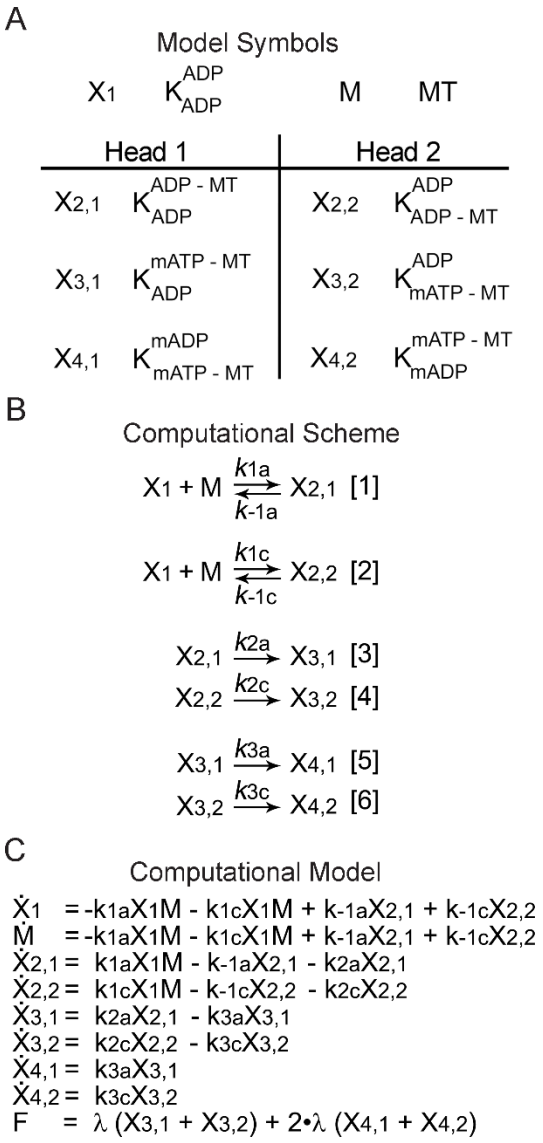


**Figure S1. Model Symbols, Computational Scheme, and Model Equations** *(A)* The model symbols are indicated. K represents the KIF3 heterodimer, and the superscript and subscript represent the nucleotide and microtubule binding states of each head. mantATP, mATP; mantADP, mADP. *(B)* The computational scheme consists of microtubule association (*reactions 1 and 2*), ADP release and mantATP binding (*reactions 3 and 4*), and the nucleotide promoted transitions from mantATP-promoted isomerization through phosphate release, dissociation, and subsequent mantATP binding (*reactions 5 and 6*). Reactions 1, 3, and 5 correspond to the KIF3A pathway, and reactions 2, 4, and 6 correspond to the KIF3C pathway. *(C)* The developed model consists of 8 ODEs representing the concentration change of each kinesin conformational state and substrate. Total fluorescence (F) was determined by summing the fluorescence emitted by the mantATP and/or mantADP bound kinesins, where concentration was converted to fluorescence using amplitude factors $\lambda$ and $2 \bullet \lambda$.

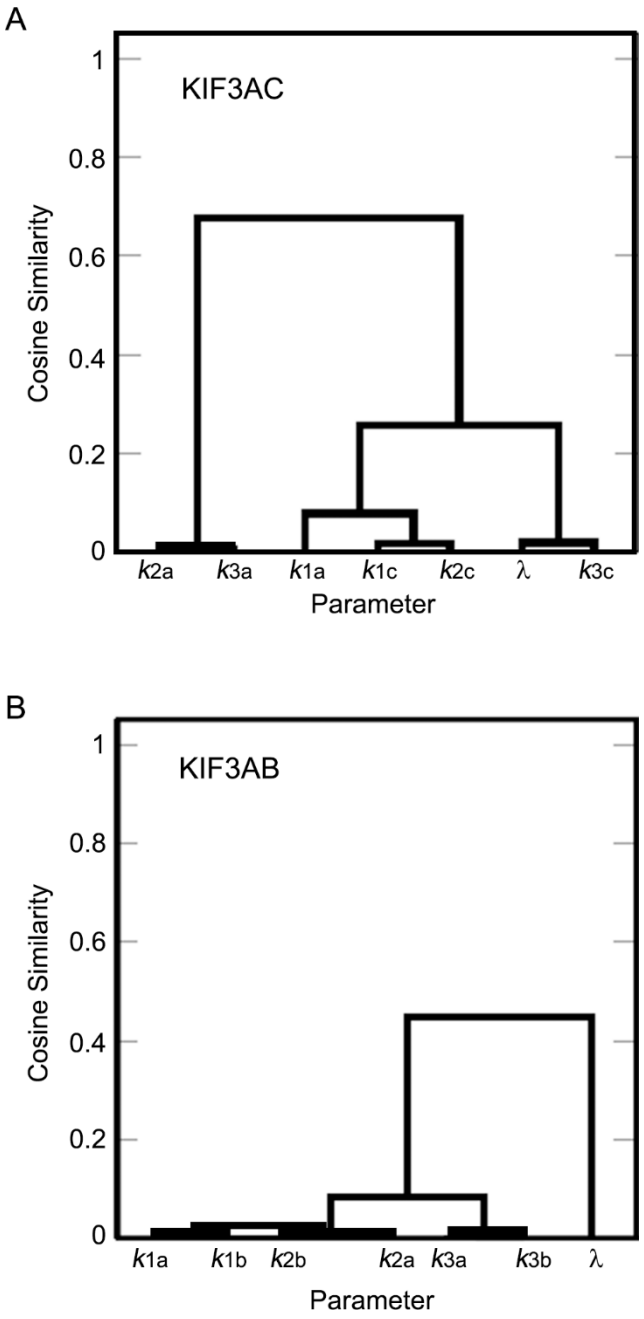


**Figure S2. KIF3AC and KIF3AB parameter correlation dendrogram.** Sensitivity analysis was conducted by calculating the sensitivity magnitude or degree to which a parameter value affects the model output, for each parameter. In addition, parameters were clustered based on the cosine distance that indicates the similarity between the parameters in a dendrogram. *(A)* The dendrogram with the clustered KIF3AC parameters and *(B)* the dendrogram with clustered KIF3AB parameters are shown. Parameters in the same branch or sub-branch are more correlated than parameters found in separate. Note that the fluorescence factor for mantATP and mantADP bound motors, was constrained as double the value of λ.

## Computational Modeling Approach and Methods

***Mathematical modeling.*** A model describing the fluorescence transients representing mantATP and/or mantADP bound KIF3AC or KIF3AB was implemented in MATLAB® (Mathworks, Inc. Natick, MA). A set of ODEs representing the kinesin or nucleotide states were derived (Fig. S1*C*). Parameter fitting of the model required the use of iterative gradient-based estimation routines where the model with the parameter estimates were solved at each iteration using numerical integration. The objective function of the estimation procedure is the mean squared error (MSE) which needed to be minimized. The MATLAB® function *fmincon* was used for solving the nonlinear programming problem, and the option of using an interior-point algorithm was chosen. The MATLAB® ODE solver for solving the model at each iteration was *ode45*. The time dependent fluorescence output for the simulations was determined by multiplying the concentrations of the species that could emit fluorescence by their respective fluorescence factors $\lambda$ or $2 \bullet \lambda$. All transients were either allocated for training to determine model parameters (i.e., fitting the model to the data) or validation to determine how well the model predicted the data not used for fitting. Parameters of the model were either taken from the literature or estimated from the data presented herein. In an effort to reduce overfitting, approximately 75% of transients were used for training, and the remaining 25% of transients were used for validation. Goodness of fit of the simulations to the fluorescence transients was determined by computing the MSE, representing the average of the sum of the squared deviations of the simulations to the experimental data. Mathematically, MSE can be given by:

$$\frac{1}{r}\sum_{i=1}^{r}(y_i - \hat{y}_i)^2 \qquad \text{(Eq. S1)}$$

where $y$ represents the experimental measurements, $\hat{y}$ represents the simulation output, $r$ represents the total number of fitted data points, and the index $i$ refers to the $i$-th measurement or predicted output corresponding to a particular time point. Simulations resulting in lower MSE values signify that the model better predicts the fluorescence transients.

### Parameter Sensitivity Analysis

Our dynamic model can be represented by a series of nonlinear ODEs as follows:

$$\begin{aligned} \frac{dx}{dt} &= f(x,p) \\ y &= g(x,p) \end{aligned} \qquad \text{(Eq. S2)}$$

where $x \in \mathbb{R}^{nx1}$ represents the state vector, $p \in \mathbb{R}^{mx1}$ represents the parameter vector, and $y$ represents the model output, i.e., the fluorescence in this case. $n$ is the number of states and $m$ equals the number of parameters. Differentiating the state with respect to the parameter yields the state sensitivity $\partial x/\partial p$:

$$\frac{d}{dt}\left(\frac{\partial x_j}{\partial p_i}\right) = \sum_{k=1}^{n}\left(\frac{\partial f_j}{\partial x_k} \bullet \frac{\partial x_k}{\partial p_i}\right) + \frac{\partial f_j}{\partial p_i} \quad \text{(Eq. S3)}$$

where $\partial x_j/\partial p_i$ refers to the sensitivity of state $j$ with respect to parameter $i$. In a similar fashion, an output sensitivity matrix $s$ can be represented as follows:

$$s = \begin{bmatrix} \frac{\partial y(t_1)}{\partial p_1} & \cdots & \frac{\partial y(t_1)}{\partial p_m} \\ \vdots & \ddots & \vdots \\ \frac{\partial y(t_h)}{\partial p_1} & \cdots & \frac{\partial y(t_h)}{\partial p_m} \end{bmatrix} \quad \text{(Eq. S4)}$$

Where $t_h$ refers to the $h$-th time point, $y$ represents the output, and $m$ is the number of parameters as stated above. The sensitivity equations were solved simultaneously with the original model equations in the scheme provided in (1).

Once the sensitivity matrix was computed, parameters were clustered in a dendrogram based on the cosine distance (d) between pairs of sensitivity vectors. Each column of the sensitivity matrix represents a vector for the output $y$ with respect to parameter $p_i$. The cosine distance is given by d = 1-|cosθ|. The angle (θ) between sensitivity vectors $a$ and $b$ corresponds to the cosine similarity. In other words, parameters were clustered based on the degree to which they are pairwise indistinguishable, i.e., the correlations of their effects on the measurements. As such, the cosine similarity is mathematically given by:

$$1 - cos(\theta_{ab}) = 1 - \frac{a \cdot b}{||a|| \cdot ||b||} \quad \text{(Eq. S5)}$$

**KIF3AC Modeling Approach**

In determining the parameter set for estimation, correlations among parameters were minimized by using a hierarchical clustering approach to group pairwise indistinguishable parameters together in a dendrogram (Fig. S2) (1). Parameters found within a branch at a low cosine similarity value (i.e. < 0.2) are highly correlated, and only a single parameter within the branch can be estimated. For example, in the KIF3AC correlation dendrogram shown in Fig. S2*A*, the KIF3A ADP release parameter ($k_{2a}$) and the parameter representing the combined series of steps thereafter for the KIF3A pathway ($k_{3a}$), are within the same branch at a cosine similarity value below the threshold of 0.2. Therefore, both parameters are indistinguishable from each other, and only one can be estimated.

A set of parameters in the KIF3AC model was determined for estimation by using the parameter correlation dendrogram as a guide (Fig. S2*A*). If a threshold cosine similarity value of 0.2 is used, the parameters can be clustered into three different branches. Branch 1 contains parameters $k_{2a}$ and

$k_{3a}$; branch 2 contains parameters $k_{1a}$, $k_{1c}$, and $k_{2c}$; and branch 3 contains λ and $k_{3c}$. Only a single parameter can be estimated from each of these branches. Parameters were sequentially eliminated from the estimation set based on their correlation with other parameters. In branch 3, it was necessary to estimate fluorescence parameter λ; therefore, parameter $k_{3c}$, which is clustered with λ and represents the combined series of steps from ATP promoted isomerization through phosphate release, dissociation, and subsequent mantATP binding in the KIF3C pathway (Fig. 1, E2-E5), could be eliminated from the parameter estimation set. In branch 1, parameter $k_{3a}$ must be estimated because $k_{3c}$ in branch 3 was eliminated from the parameter estimation set. Next, parameter $k_{2a}$ in branch 1, which corresponds to KIF3A ADP release, must not be estimated because it is clustered with parameter $k_{3a}$ which was selected for estimation. Finally, in branch 2, the KIF3A microtubule association parameter ($k_{1a}$) was selected, and the other parameters in the branch had to be eliminated from the parameter set for estimation due to their high correlation.

Both ADP release parameters for the two heads were set to their intrinsic, or nominal, rates for the simulations, and an alternative model where ADP release by KIF3A and KIF3C is similar was ruled out (Table S1 and Table S2). In total, three out of the seven parameters ($k_{1a}$, $k_{3a}$, and λ) were selected for estimation, and their confidence intervals were determined using a profile likelihood estimation approach (2). The KIF3AC parameters served as constraints which were then used to determine parameters $k_{1c}$ and $k_{3c}$ (Table S1). Parameter λ served as a factor for the conversion of the concentration of KIF3•mantATP, KIF3•mantADP, and KIF3•mantADP•Pi intermediates to fluorescence emission. The factor for the conversion of mant-nucleotide saturated kinesins to fluorescence emission was 2•λ. Therefore, only a single fluorescence parameter λ is presented in the dendrogram. Parameters not selected for estimation were set to their nominal or intrinsic values, and therefore, confidence intervals cannot be determined for these parameters.

Parameter estimation for the KIF3AC model required several constraints representing the model assumptions (Table S1). For KIF3AC, microtubule association was assumed to be represented by the sum of the parameters of the two heads; therefore, one constraint was that the sum of the microtubule association parameters for KIF3A and KIF3C had to equal the KIF3AC parameter of 6.6 $\mu M^{-1}s^{-1}$. The nominal microtubule association rates assigned to KIF3A and KIF3C were 5.7 $\mu M^{-1}s^{-1}$ and 1 $\mu M^{-1}s^{-1}$, respectively. These rates represent half of the KIF3AA and KIF3CC rate constants because microtubule association was assumed to be represented by the sum of the rates for the two heads.

Downstream of microtubule association, the average of the rates for the steps in the KIF3A and KIF3C pathways was assumed to equal the KIF3AC parameters. The KIF3AA ADP release rate of 77.7 $s^{-1}$ and KIF3CC rate of 7.6 $s^{-1}$ were assigned as nominal values to KIF3A and KIF3C, respectively. The average of these nominal parameter values results in a rate resembling that for KIF3AC at 42.5 $s^{-1}$. If the cosine similarity threshold value is decreased to ~0.1, and the ADP release parameters are included in the parameter estimation set, there is very little change from their nominal values; therefore, the ADP release parameters were fixed and not selected for estimation.

For the combined steps downstream of entry into the processive run (Fig. 1*A*, E2-E5), the rates have not been determined for KIF3AA, KIF3CC, and KIF3AC. However, the steady-state $k_{cat}$ for

KIF3CC is ~1 $s^{-1}$, which suggests that there is a slow step between mantATP promoted isomerization and coupled phosphate release and dissociation (Fig. 1, E2-E5). Therefore, the nominal value assigned to parameter $k_{3c}$ for the KIF3C pathway was slow at 1 $s^{-1}$. In contrast, because KIF3A is intrinsically fast, the nominal value assigned to parameter $k_{3a}$ for the KIF3A pathway was fast at ~100 $s^{-1}$. The average of these nominal $k_{3a}$ and $k_{3c}$ parameter values is 50 $s^{-1}$. Therefore, for parameter estimation, the average of parameter $k_{3a}$ and $k_{3c}$ for combined steps E2-E5 in the two pathways had to equal ~50 $s^{-1}$. Finally, the nominal parameter values for the KIF3A and KIF3C pathways served as the bounds for the range of possible values for each kinetic parameter during estimation. For fluorescence parameter λ, possible values could range from 0.0001 to 100. In order to ensure that a global minimum was reached, a multi-start approach was implemented where randomized sets of nominal values were assigned to the parameters being estimated for each head. The simulations consistently produced similar parameter values as presented in Table 2, confirming that a global minimum was reached. The validity of all model conditions was assessed, and a detailed explanation of why they were declared valid or not valid is presented in Table S1 and Table S2.

**KIF3AB Modeling Approach**

A set of parameters was also selected for estimation for the KIF3AB model. The parameter correlation dendrogram for KIF3AB (Fig. S2*B*) showed that most of the model parameters were highly correlated with each other. When a threshold cosine similarity value of 0.2 is applied to the dendrogram, the parameters can be clustered into two branches. Branch 1 contains all kinetic parameters ($k_{1a}$, $k_{1b}$, $k_{2a}$, $k_{2b}$, $k_{3a}$, and $k_{3b}$) and branch 2 contains fluorescence parameter λ. Because of the high correlation among the kinetic parameters for KIF3AB, a different approach for parameter selection and estimation was necessary. The catalytic properties of KIF3A and KIF3B are similar in KIF3AA and KIF3BB (Table 1); therefore, it was assumed that KIF3A and KIF3B likely have similar properties in KIF3AB. This assumption reduced the number of parameters for estimation and therefore simplified the modeling. In addition, since the KIF3AC model predicted that KIF3A and KIF3C microtubule association properties were similar whereas both heads retained their intrinsic ADP release properties, the microtubule association parameters in the KIF3AB model were first selected for estimation, and the ADP release parameters for the two heads were fixed to their intrinsic values. These model conditions were proven to be valid, and alternative model conditions were systematically excluded (Table S3). However, the parameters for the combined series of nucleotide dependent transitions downstream of ADP release during entry into the processive run for the KIF3A and KIF3B pathways (Fig 1*A*, E2-E5) were unknown. Because only a single kinetic parameter could be estimated at a time due to the high correlation among the parameters, a sequential estimation approach was implemented. First, the $k_3$ parameters were fixed at a value of 50 $s^{-1}$ that served as an initial estimate while the microtubule association parameters were estimated in the first round of simulations. When the estimated parameters for microtubule association for the two heads were summed, the resulting KIF3AB microtubule association rate constant was consistent with previous studies (3). In the second round of simulations, the microtubule association parameters were fixed to the values estimated from the first round of simulations, and the $k_3$ parameters were selected for estimation. The values for parameters $k_{1a}$, $k_{1b}$, $k_{2a}$, and $k_{2b}$ could not exceed the intrinsic or nominal values for the parameters. The lower bound for the possible values for the parameters had to be sufficiently small (i.e. one-

hundredth the nominal value). Likewise, for parameters $k_{3a}$ and $k_{3b}$, the lower bound had to be sufficiently small (i.e. one-hundredth the nominal value) and values could not exceed 100 $s^{-1}$. The bounds for possible values for fluorescence parameter λ were 0.0001 to 100. The resulting set of parameter values for KIF3AB are presented in Table 2. A multi-start approached confirmed that a global minimum, as opposed to a local minimum, had been reached.

**Parameter Estimation**

The parameter estimation problem used for modeling all fluorescence transients can be mathematically represented as follows:

$$\min_{p} \sum_{i} \sum_{k} (y_{ik} - \hat{y}_{ik})^2 \qquad \text{(Eq. S6)}$$

where $y_{ik}$ and $\hat{y}_{ik}$ represent the simulated and measured fluorescence, respectively of the $i_{\text{th}}$ experimental condition at the $k_{\text{th}}$ time. The fluorescence was computed at 1000 different time points spanning the interval 0-0.5 seconds for experiments with KIF3AC or 0-0.2 seconds for experiments with KIF3AB. The parameters ($p$) were $k_{1a}$, $k_{1c}$, $k_{2a}$, $k_{2c}$, $k_{3a}$, $k_{3c}$, and λ. λ represents the fluorescence amplitude of KIF3 bound to a single mantATP or mantADP, and 2•λ represents the fluorescence amplitude for KIF3 bound to mantATP and mantADP. The optimization option chosen for *fmincon* was an interior-point algorithm. In order to determine parameter confidence intervals, a widely used profile likelihood approach was implemented (2). For each estimated parameter, the profile likelihood was determined by fixing the parameter to a range of rates while reoptimizing the other parameters. The confidence level used for this procedure was 95%, and the corresponding chi square critical value of 3.8 for one degree of freedom served as the confidence threshold. More information regarding the profile likelihood technique can be found in (2).

**Supporting References**


1. Dai, W., Bansal, L., Hahn, J., and Word, D. (2014) Parameter set selection for dynamic systems under uncertainty via dynamic optimization and hierarchical clustering. *Aiche J* **60**, 181-192
2. Kreutz, C., Raue, A., Kaschek, D., and Timmer, J. (2013) Profile likelihood in systems biology. *Febs J* **280**, 2564-2571
3. Albracht, C. D., Guzik-Lendrum, S., Rayment, I., and Gilbert, S. P. (2016) Heterodimerization of kinesin-2 KIF3AB modulates entry into the processive run. *J Biol Chem* **291**, 23248-23256